




Assessment of TiO₂ and Ag/TiO₂ photocatalysts for domestic wastewater treatment: synthesis, characterization, and degradation kinetics analysis

Rogelio Estrada-Vázquez¹ · Mabel Vaca-Mier² · Victoria Bustos-Terrones³ · Jesús Gabriel Rangel-Peraza¹ · Juan G. Loaiza¹ · Yaneth A. Bustos-Terrones⁴ 

Received: 31 October 2023 / Accepted: 19 December 2023 / Published online: 26 December 2023
© Akadémiai Kiadó, Budapest, Hungary 2023

Abstract

In this study, the synthesis and characterization of the TiO₂ and Ag/TiO₂ nanoparticles were carried out and their influence on the oxidation of organic matter of domestic wastewater was evaluated using a heterogeneous photocatalytic system. The TiO₂ and Ag/TiO₂ nanoparticles were synthesized by the sol–gel method and the chemical reduction method. The nanoparticles were characterized by four different techniques (X-ray diffractometry, UV–Vis spectrophotometry, Fourier transform infrared spectroscopy, and scanning electron microscopy). The importance of the synthesized nanoparticles in the treatment of residual water was evaluated using a photocatalysis process with UV light ($\lambda=254$ nm). Raw domestic wastewater generated at the local university was used. Due to the complexity of the wastewater composition, the Chemical Oxygen Demand (COD) was used to evaluate the oxidation of organic matter in the photocatalytic system. Three different concentrations of TiO₂ and Ag/TiO₂ were evaluated: 0.25, 0.5 and 1 g L⁻¹. The photocatalysis process achieved a maximum degradation of 68% and 77% when using TiO₂ and Ag/TiO₂ after 2 h operation. A maximum kinetic rate value of 0.013 min⁻¹ was obtained when Ag/TiO₂ was used as a catalyst, like the observed in other advanced oxidation processes.

✉ Yaneth A. Bustos-Terrones
yaneth.bt@culiacan.tecnm.mx

¹ División de Estudios de Posgrado e Investigación, TecNM-Instituto Tecnológico de Culiacán, Juan de Dios Bátiz, No. 310. Col. Guadalupe, 80220 Culiacán, Sinaloa, Mexico

² Universidad Autónoma Metropolitana, Ciencias Básicas e Ingeniería, San Pablo, No. 180. Col. Reynosa Tamaulipas, Azcapotzalco, 02200 Mexico City, CDMX, Mexico

³ Dirección Académica de Ingeniería en Tecnología Ambiental, Universidad Politécnica del Estado de Morelos, Boulevard Cuauhnáhuac, No. 556. Col. Lomas del Texcal, 62550 Jiutepec, Morelos, Mexico

⁴ División de Estudios de Posgrado e Investigación, CONAHCYT-TecNM-Instituto Tecnológico de Culiacán, Juan de Dios Bátiz, No. 310. Col. Guadalupe, 80220 Culiacán, Sinaloa, Mexico

Keywords Photocatalysis · TiO_2 · Ag/TiO_2 · Wastewater · UV light

Introduction

Water is the most important resource in human life and most activities that use water generate wastewater. Novel technologies have been proposed for wastewater treatment, among which the photocatalytic oxidation treatment stands out [1]. Heterogeneous photocatalysis has proven to be effective for the degradation of pollutants [2, 3]. Due to its semiconductor properties, TiO_2 in its anatase phase has been widely studied since its photocatalytic activity is present in the ultraviolet UV–visible region [4, 5].

TiO_2 has been used for over 20 years for the degradation of several pollutants in the photocatalysis process. The use of TiO_2 as a catalyst in photocatalysis processes has continued to be prevalent and relevant in recent years due to its efficiency, versatility, low cost, environmental friendliness, and stability [6, 7]. Recent studies report the modification of the TiO_2 surface, explore different doping techniques, and develop composite materials to enhance photocatalytic properties. An example of these advancements is Losada et al. [8], who evaluated the treatment of a mixture of azo dyes by photocatalysis with TiO_2 in suspension using sunlight and artificial light. The artificial light system showed that the concentration of dyes and TiO_2 were the most important factors that influenced the removal of color and COD. The photocatalytic system with sunlight removed 100% of color and 80% of COD after 3 h of treatment, demonstrating the degradative capacity of the photocatalytic system with TiO_2 and sunlight. Fernández et al. [9] evaluated TiO_2/UV photocatalysis for wastewater treatment using thin films. They used a simple method of gravity sedimentation on a glass substrate for the preparation of the films. Photocatalytic assays using TiO_2 films generated 99.5% discoloration, 79% removal of total organic carbon, and a total microbial inactivation after 14 h of treatment.

Some researchers have shown that a photocatalytic treatment of water can be improved if the catalyst is doped. Dodoo-Arhin et al. [10] synthesized TiO_2 particles through sol–gel methods and hydrothermal procedures. They evaluated synthesized TiO_2 nanostructures as catalysts for the photocatalytic decomposition of synthetic dyes in a batch reactor with ultraviolet light. The results showed a 100% decomposition of Sudan III dye when using a hydrothermal catalyst, while a 94% decomposition of rhodamine B dye was shown when using a catalyst synthesized by the sol–gel method. Castillo-Ledezma et al. [2] demonstrated the photocatalytic effectiveness of the nitrogen-doped TiO_2 catalyst for the inactivation of *Escherichia coli* in aqueous suspensions under complete irradiation of solar spectra. They evaluated the effect of pH, type of irradiation, and concentration of TiO_2 doped with nitrogen. The treatment was improved when the nitrogen-doped photocatalyst was added to the solution. The acidic conditions were demonstrated as the most favorable conditions for disinfection. Bibi et al. [11] used a solvothermal method with a bioreactor to synthesize a mesoporous TiO_2 membrane doped with Cu (1–3% by weight). The resulting nanomaterials were analyzed using various techniques, including X-ray diffractometry (XRD), field emission scanning electron microscopy (FESEM),

Fourier-transform infrared spectroscopy (FTIR), energy-dispersive X-ray spectroscopy (EDS), and cyclic voltammetry (CV). Cu doping altered the light absorption towards the visible spectrum and achieved a lower bandgap energy (2.6 eV) compared to pure TiO₂ (3.2 eV). Cu-doped photocatalysts exhibited a photocatalytic performance of 99% in the degradation of red Congo, higher than the effectiveness observed for pure TiO₂. Cyclic voltammetry detected active species, such as Cu²⁺ and Cu¹⁺, when using the Cu⁻-doped nanocatalyst. Oxygen vacancies and the electronegative surface of Cu¹⁺ played a crucial role in the photocatalytic reduction of red Congo.

An efficient application of heterogeneous photocatalysis with TiO₂ requires the use of nanoparticles [12]. Wang et al. [13] successfully synthesized boron and/or cerium-doped nanomaterials using the sol–gel method. As a result, the boron and cerium ions doped with TiO₂ favored the photocatalytic antimicrobial activity. The ion-doped TiO₂ showed a small crystal size with a high specific surface area, which favored the disinfection treatment. Wang et al. [14] synthesized a series of carbon and boron ion-doped TiO₂ nanomaterials to improve the microbial activity of the nanomaterial. The results showed that the carbon and boron-doped TiO₂ nanomaterial improved antibacterial activities under visible light irradiation in comparison with simple TiO₂ nanomaterial.

Several photocatalytic studies have been reported for the removal of organic matter, but most of these investigations have been carried out in synthetic wastewater where a sole analyte of interest is used (azo dyes, antibiotics, pesticides, among others). This study proposed the use of TiO₂ and Ag/TiO₂ nanoparticles as catalysts for the treatment of domestic wastewater (Table 1). The material was synthesized and characterized. The use of the synthesized nanoparticles in the treatment of wastewater was evaluated using a heterogeneous photocatalysis process under UV–C (wavelength = 254 nm) light irradiation. Both TiO₂ and Ag/TiO₂ photocatalytic systems were compared based on the removal efficiencies and degradation rates.

Materials and methods

Materials

All the reagents used in the work were of reagent-grade quality (Sigma Aldrich or JT Baker). For the synthesis of TiO₂ and Ag/TiO₂ nanoparticles, titanium isopropoxide (C₁₂H₂₈O₄Ti), ethanol (CH₃CH₂OH), hydrochloric acid (HCl), silver nitrate (AgNO₃), sodium borohydride (NaBH₄), and sodium citrate were used (Na₃C₆O₇H₅).

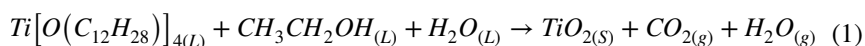
Synthesis of nanoparticles

The Sol–Gel method is a method that is widely applied in the science of nanomaterials [21]. Titanium isopropoxide was used as a precursor and hydrolyzed under mixing, by adding ethanol and hydrochloric acid. For the synthesis of TiO₂

Table 1 Summary of pollutant removal processes by photocatalysis with TiO₂ as a catalyst

Catalyst	Contaminant removed	Irradiation type	Removal (%)	Time (min)	Ref
TiO ₂ /N nanoparticles	<i>E. Coli</i>	Sunlight spectra	–	60	Castillo-Ledezma et al. [2]
Mesoporous TiO ₂ Nanoparticles	Rhodamine B Sudan III	UV-A light	94% Rhodamine 100% Sudan	120	Dodoo-Arthin et al. [10]
TiO ₂ nanoparticles	Azo dyes	Sunlight spectra	100% Color 80% COD	180	Losada et al. [8]
TiO ₂ /Ag Nanofibers	Azo dyes	Visible light	99.5% Methyl Orange 92% Rhodamine 99% Methylene blue	240	Wang et al. [15]
TiO ₂ biofilms	Microbiology wastewater	UV-C light	79% TOC 100% Microbial inactivation	840 min	Fernández et al. [9]
TiO ₂ /Ag nanoparticles	Azo dyes	Visible light	95% Rhodamine 76% Methylene blue 23% Methyl orange	330	Ghosh et al. [16]
Ag/TiO ₂ beads	Cr (VI)	UV light (unspecified UV region)	5 PPM	15	Athanasekou et al. [17]
TiO ₂ nanoparticles	Methylene blue	UV light (unspecified UV region)	90.5%	30	Subekti and Helmiyati, [18]
Films of TiO ₂ and Ag/TiO ₂	Fecal coliforms	UV-A light	100%	6	Dominguez-Espindola et al. [19]
TiO ₂ /Pd	Methylene blue Methyl orange	UV light (unspecified UV region)	100% Color 77.1% Methyl orange 85.9% Methylene blue	180	Nguyen et al. [20]
TiO ₂ and Ag/TiO ₂ nanoparticles	Domestic wastewater	UV-C light	76.95% COD	120	This Work

nanoparticles, 15 mL of Titanium Isopropoxide was added to 15 mL of ethanol. Then 10 mL of distilled water was added dropwise while the system was kept stirring for about 10 min. Equation 1 describes the formation mechanism of TiO₂ nanoparticles. Finally, 0.5 mL of hydrochloric acid was added in a concentration of 0.1 M. The system was heated to 70 °C (being careful not to exceed this temperature) until the residual water evaporated. The obtained TiO₂ was placed in a ceramic crucible and then put into an oven with temperature conditions of 100 °C to dry it. Subsequently, a heat treatment was applied at 500 °C for 2 h using a digital muffle (Felisa), with a temperature ramp of 5 °C min⁻¹, starting from the ambient temperature. Ethanol was used for controlling the rate of hydrolysis, while hydrochloric acid worked as a catalyst, obtaining acid catalysis [22].



The synthesis of Ag/TiO₂ was implemented using the chemical reduction method, with a slight modification of the Turkevitch method [23, 24]. Silver nitrate was used as the initial reagent and sodium borohydride as the reducing agent. Three solutions were prepared: silver nitrate at 2.5 mM L⁻¹, sodium citrate at 2.5 mM L⁻¹, and sodium borohydride at 10 mM concentrations. 100 mL of silver nitrate was mixed with 100 mL of sodium citrate while stirring for at least 5 min. Then 3 mL of sodium borohydride was added and continuous stirring was implemented until a color change was obtained in the final solution. TiO₂ synthesized with the Sol–Gel method was recovered and placed in a crucible adding the silver solution drop by drop until covering the entire surface of the TiO₂. The ceramic crucible was placed into an oven under temperature conditions of 100 °C until dry. Finally, a heat treatment was applied at 500 °C for 2 h.

Characterization

An X-ray diffractor (Bruker) equipped with a radiation copper target ($\lambda = 1.54184 \text{ \AA}$) was used to measure the crystallinity and determine the phases present in the synthesized material. The UV absorption properties of the materials were determined through a UV–Vis spectrophotometer (Genesy 10 s) in a wavelength range of 200–600 nm. Infrared spectra were measured on an FTIR spectroscope (Nicolet iS50) in a wavelength range of 4000–500 cm⁻¹. Finally, the morphology of the nanomaterials was observed using a scanning electron microscope (SEM 200 FEI Nova). The study of the nanoparticle size was carried out by estimating the average crystal size using the Scherrer equation (Eq. 2) [24].

$$\beta = \frac{k \times \lambda}{FWHM(S) \times \cos\theta} \quad (2)$$

Here β is the average crystal size (nm); K is the factor of the crystal; λ is the wavelength of radiation used (λ_{Cu}) (nm); θ is the diffraction peak position; FWHM (S) is the width at the mean height of the sample diffraction peak.

Sampling and wastewater

The residual water was sampled from the drainage system of the local university. Composite samples were taken at 3 h intervals according to the APHA methodology [25]. Characterization of the wastewater was carried out and five physicochemical parameters were evaluated: chemical oxygen demand (COD) using the colorimetric method (Hach DR-3900 spectrophotometer), total suspended solids (TSS) (multiparametric Hach HQ30d), salinity (multiparametric Hach HQ30d), conductivity (Hach HQ30d multiparameter), temperature (Hach HQ30d multiparameter).

The wastewater did not present any previous treatment since it was taken directly from the public sewer. According to this, a pre-treatment was carried out to reduce the solids in wastewater and their possible influence on heterogeneous catalysis. This pre-treatment consisted of passing the wastewater through a filter comprised of zeolite, anthracite, and activated carbon packed in a tubular reactor. These materials were selected due to their high degree of porosity and high internal surface [1].

Photocatalytic treatment

The oxidation efficiency of contaminants was evaluated through a heterogeneous photocatalysis process with TiO_2 and Ag/TiO_2 nanoparticles, with UV-C light as the source of irradiation [26]. UV-C irradiation was chosen since this source has higher energy compared to UV-A and UV-B sources. According to this, a higher photocatalytic activity can be achieved and a faster and more efficient degradation of pollutants can be obtained. Besides, when UV-C is combined with photocatalysis, this process can provide simultaneous pollutant degradation and microbial inactivation [27, 28]. However, UV-C radiation sources are more expensive since specific equipment and infrastructure are required to generate and control the light output contrary to UV-A and UV-B sources that are readily available since they are part of solar radiation [29, 30]. Three catalyst concentrations were selected based on the reported in the literature [2]. An ultraviolet lamp with a wavelength ($\lambda=254$ nm) was used in a tubular reactor with a capacity of 250 mL. After the catalyst and wastewater were added to the reactor, heterogeneous catalysis was induced. The main purpose of photocatalytic treatment was to remove organic matter, which was measured as Chemical Oxygen Demand (COD).

Organic matter removal

The removal efficiency (RE) of organic matter was calculated after implementing the wastewater treatment through the photocatalysis process [31]. The Removal efficiency was determined with the following Eq. 3:

$$\text{RE}(\%) = \left(\frac{C_0 - C_f}{C_0} \right) \times 100 \quad (3)$$

Here C_0 is the input pollutant load (mg L^{-1}); C_f is the output pollutant load (mg L^{-1}) at time (t).

Photocatalytic degradation kinetics

A regression analysis was conducted to examine the kinetic model data using the Langmuir–Hinshelwood (L–H) model. The mathematical expression corresponding to this model is [32]:

$$r = -\frac{dc}{dt}k_r\theta = \frac{k_rKC}{1 + KC} \quad (4)$$

Here r is the reaction rate, k_r is the reaction rate constant, K is the reactant adsorption constant, θ is the fraction of the surface of TiO_2 , and C is the concentration of organic matter at any time (t). Equation 4 can be simplified to a pseudo-first-order kinetic model as Eq. 5:

$$r = -\frac{d_c}{d_t}k_rKC = k_0t \quad (5)$$

Here $k_0 = k_r K$.

Equation 5 can be solved and linearized as shown in Eq. 6:

$$\ln \frac{C_0}{C} = k_0t \quad (6)$$

According to Lente [33] and Estrada-Vázquez et al. [34], linearization methods are outdated now in chemical kinetics, and non-linear least squares fitting to the untransformed original equation should be used. Therefore, the photocatalytic degradation kinetics are described by the first-order exponential model following the Eq. 7:

$$C = C_0 * e^{-kt} \quad (7)$$

Here C is the organic matter concentration, (mg L^{-1}) and k represents the first-order kinetic constant, (min^{-1}) through time. Kinetic constants were obtained for all treatments carried out in the photocatalysis process with TiO_2 and Ag/TiO_2 nanoparticles.

Statistical analysis

The treatments were carried out at five different times in quadruplicate within a time range of 2 h. Statistical analysis was performed using removal efficiencies and kinetic constants as response variables. An analysis of variance was carried out to compare the photocatalysis processes with TiO_2 and Ag/TiO_2 nanoparticles. This statistical analysis was also used to figure out the effect of catalyst concentration on the removal efficiencies and kinetic rates. The software used for data analysis was Statgraphics.

Results and discussion

TiO₂ and Ag/TiO₂ nanoparticles

The Sol–Gel synthesis method allowed the manipulation of the material at the molecular level [21]. In this study, high-purity materials were synthesized to control the characteristics of the microstructure. Ag/TiO₂ nanoparticles were obtained by the chemical reduction method using a modification of the Turkevitch method, which is frequently used to synthesize gold particles [23]. The reaction that allowed obtaining these nanoparticles is shown in Fig. S1.

Characterization of TiO₂ and Ag/TiO₂ nanoparticles

X-ray patterns were recorded in a range of 2θ between 10° and 100° . Fig. 1a shows that TiO₂ exhibited an anatase phase at the diffraction peak $2\theta = 25^\circ$ [34–36]. This peak could be related to the predominant homogeneous crystalline phase, which is consistent with the one reported by other researchers [4, 13]. Furthermore, the presence of TiO₂ in the anatase phase coincides with the diffraction pattern obtained when the X-ray diffractometer was equipped with a copper target of $\lambda = 1.54184 \text{ \AA}$. Fig. 1b shows the diffractogram of the Ag/TiO₂ nanoparticles. TiO₂ exhibited an anatase phase at $2\theta = 25^\circ$ as the predominant homogeneous crystalline phase, while silver (Ag) was found at $2\theta = 35^\circ - 40^\circ$. This situation is similar to the one reported by other researchers [37, 38]. Likewise, the deposition of silver nanoparticles is related to changes in the size of the crystallographic peaks. This is because silver nanoparticles, being smaller, can enter the interstitial sites of the crystalline structure of TiO₂ in its anatase phase and consequently increase the volume of the unit cell [5]. Based on X-ray characterization, the average crystal size was determined using the Scherrer equation. As a result, nano-sized crystals were synthesized with an average of 1.421 nm for the case of TiO₂, and for the Ag particles, the nano-size of the crystal was on average 0.507 nm.

Silver solutions were analyzed using a UV–Vis spectrophotometer. The absorbance of the solutions was measured in the 200–600 wavelength spectrum range. Measurements were carried out immediately after the synthesis procedure. Fig. S1 shows the images of the silver (Ag) colloids that were prepared to obtain the synthesized nanoparticles. Fig. 2 shows the UV–Vis spectra of Ag colloids, obtained from varying the Ag proportion in six different solutions prepared (0.06, 0.08, 0.10, 0.12, 0.14, 0.16 mM). The spectrum of synthesized silver nanoparticles was very similar to those reported by Pinto et al. [39] where a λ_{max} was present close to 400 nm.

Fourier transform infrared spectroscopy (FTIR)

The FTIR spectra of TiO₂, Ag, and Ag/TiO₂ in a frequency range of 4000–500 cm^{-1} are shown in Fig. 3. The peaks below 500 cm^{-1} correspond to the

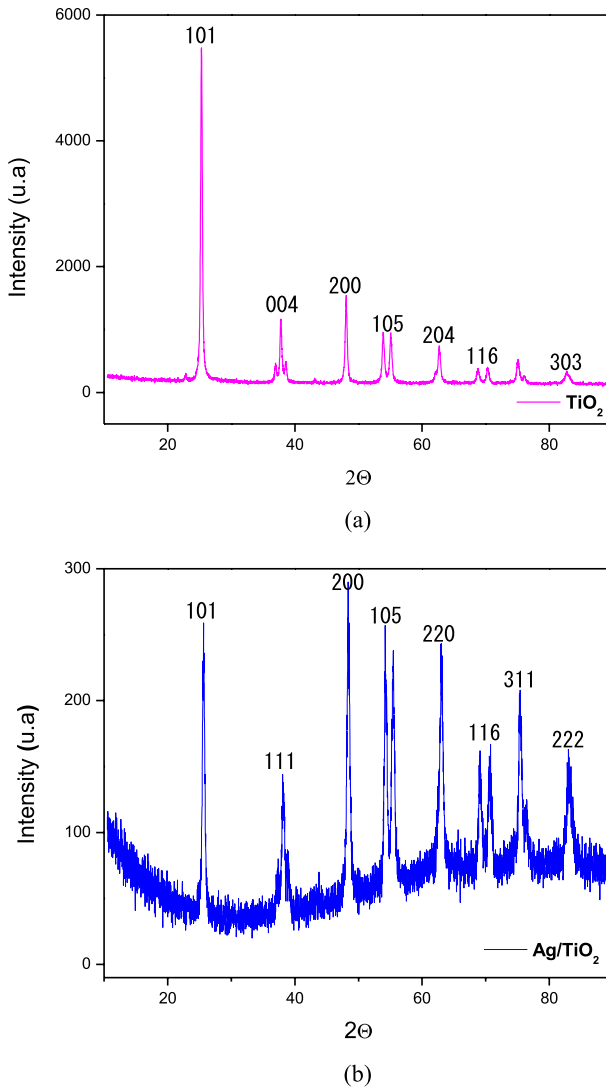


Fig. 1 Nanoparticle diffractogram of **a** TiO_2 and **b** Ag/TiO_2 . X-ray pattern range = 2θ (10° – 90°). $\text{Cu K}\alpha$ radiation target ($\lambda = 1.54184$ nm).

vibrations of TiO_2 and Ag/TiO_2 . The presence of these bands indicates that the structure of the TiO_2 nanoparticles is maintained and that the Ag nanoparticles only cover them. This behavior coincides with the reported by some researchers [8, 40]. An FTIR spectrum peak around 3300 cm^{-1} is also shown, which is attributed to the OH stretching mode of the surface and the adsorbed water molecules, this is consistent with that reported by Xue et al. [5] The spectrum also revealed

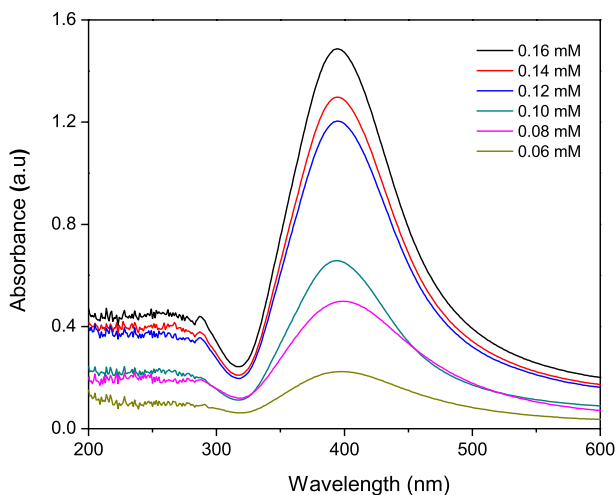


Fig. 2 UV-Vis absorption spectrum of Ag nanoparticles at different concentrations. Wavelength spectra range 200–600 nm. Silver colloid (Ag) concentrations: –Ag (0.16 mM), –Ag (0.14 mM), –Ag (0.12 mM), –Ag (0.10 mM), –Ag (0.08 mM), –Ag (0.06 mM)

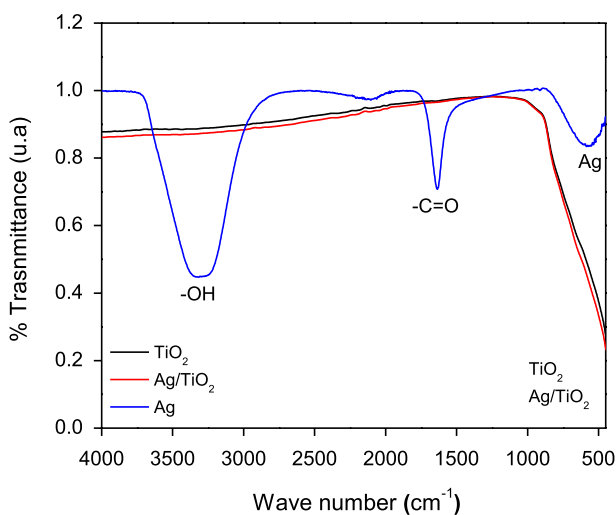


Fig. 3 FTIR spectra of TiO₂, Ag/TiO₂, and Ag. Spectrum frequency range 4000–500 cm⁻¹. Nanoparticles: –TiO₂, –Ag/TiO₂, –Ag

absorption bands at 1600 cm^{-1} belonging to the C=O bond vibrational vibrations [41, 42].

Scanning electron microscopy (SEM)

The morphology of the synthesized TiO_2 nanoparticles was analyzed by scanning electron microscopy. Fig. S2 shows small-sized, spherical nanoparticles smaller than the 50 nm range. The resolution was expanded showing that the nanoparticles are smaller than a range of 20 nm. The TiO_2 nanoparticles exhibited a non-uniform particle shape due to particle agglomeration. The structure of TiO_2 nanoparticles is consistent with the reported by Haider et al. [43].

Removal efficiency

An initial characterization of the wastewater was carried out through five physico-chemical parameters of water quality. The residual water presented the following characteristics: chemical oxygen demand 173.15 mg L^{-1} ; total suspended solids 146.9 mg L^{-1} ; salinity 0.6 mg L^{-1} ; conductivity $379\text{ }\mu\text{S cm}^{-1}$; temperature $25\text{ }^\circ\text{C}$ and pH 7.6. Likewise, suspended particles were observed, which require pretreatment before the photocatalysis treatment is implemented.

A pretreatment system was carried out to remove solids present in wastewater. Three different types of filter materials were used: activated carbon (636 cm^3), zeolite (477 cm^3), and anthracite (223 cm^3). This pretreatment showed a high retention capacity of solids because 53.67 mg L^{-1} of the total suspended solids were removed. The pretreatment system also removed 31% of the organic matter

Table 2 Summary of results obtained in the photocatalysis process with TiO_2 and Ag/TiO_2

Time (Min)	[0.25 g L ⁻¹]		[0.5 g L ⁻¹]		[1.0 g L ⁻¹]	
	COD (mg L ⁻¹)	Removal efficiency (%)	COD (mg L ⁻¹)	Removal efficiency (%)	COD (mg L ⁻¹)	Removal efficiency (%)
Photocatalysis with TiO_2						
0	124	0	116.42	0	132.18	0
30	95	23.3870	84.9	27.0743	99	25.1021
60	71	42.7419	60.14	48.3422	63	52.3377
90	62	50	52.26	55.1108	51	61.4162
120	58	53.2258	48.38	58.4435	42	68.2251
Photocatalysis with Ag/TiO_2						
0	124	0	116.42	0	132.18	0
30	87	29.83	79.8	31.45	91.3	30.92
60	62	50	56	51.89	56.6	57.17
90	54	56.45	45.4	61	40.3	69.51
120	49	60.48	37.6	67.70	30.46	76.95

present in the wastewater, where the initial COD concentration of 173.15 mg L^{-1} decreased to 119.48 mg L^{-1} . Then, three different concentrations of catalyst were used and the removal efficiency of the photocatalysis system was measured after operating for 120 min. Ultraviolet light was used as a source of irradiation in this photocatalytic system, this type of light corresponds to the UV-C region with a wavelength of $\lambda=254 \text{ nm}$. Likewise, all the experiments were evaluated in the dark, to avoid the light from outside could interfere with the process. The concentrations used were: 0.25 g L^{-1} , 0.5 g L^{-1} , and 1 g L^{-1} for both TiO_2 and Ag/TiO_2 nanoparticle systems (Table 2).

The photocatalysis system using TiO_2 nanoparticles removed 53.22% of organic matter present in the wastewater when using the concentration of 0.25 g L^{-1} of catalyst. A slight increase in organic matter removal was observed when a concentration of 0.5 g L^{-1} of catalyst was used, where a removal efficiency of 58.44% was observed. However, the highest removal efficiency was observed when the photocatalysis system used a TiO_2 concentration of 1 g L^{-1} . Under this catalyst concentration, a COD reduction from 132.18 mg L^{-1} to 42 mg L^{-1} was observed in the wastewater, which represented an organic matter removal efficiency of 68.22% (Fig. 4a).

The lowest value of removal efficiency (60.48%) of the Ag/TiO_2 photocatalysis system was observed when a concentration of 0.25 g L^{-1} of catalyst was used. A similar positive trend was observed for the organic matter removal efficiency when higher concentrations of catalyst were used. Removal efficiencies of 67.70% and 76.95% were observed when Ag/TiO_2 concentrations of 0.5 g L^{-1} and 1 g L^{-1} were used in the photocatalytic system (Fig. 4b). This can be attributed mainly to the average size of the nanoparticles since the Ag/TiO_2 nanoparticles are smaller than the TiO_2 nanoparticles. Therefore, they have a greater surface area that is in direct contact with the aqueous medium (domestic wastewater) allowing greater degradation when irradiated with ultraviolet light as a source of energy.

Tables 3 and 4 present a statistical summary of all the treatments carried out in the photocatalytic system with TiO_2 and Ag/TiO_2 nanoparticles. Then, an analysis of variance was carried out to demonstrate the differences between the TiO_2 and Ag/TiO_2 photocatalysis processes (Table 5). Based on the statistical analysis, the Ag/TiO_2 process showed a higher removal efficiency of organic matter ($p < 0.05$) (Fig. 5a). The multiple range test using the LSD method also demonstrated that, in both processes, the use of a higher concentration of catalyst statistically improved the removal efficiency (Fig. 5b).

In particular, the use of the highest catalyst concentration (1.0 g L^{-1}) showed the highest organic matter removal efficiencies for both photocatalytic processes. However, the use of Ag/TiO_2 showed a statistically higher removal efficiency ($p < 0.05$) than the process that used pure TiO_2 , with mean removal efficiency values of 76.93% and 68.23%. The statistical analysis also demonstrated the reliability and repeatability of the experiments ($p > 0.05$). The removal efficiencies obtained were similar to those reported by Dodoo-Arhin et al. [10] who synthesized TiO_2 nanoparticles in the UV-assisted decomposition of a wide range of dye contaminants.

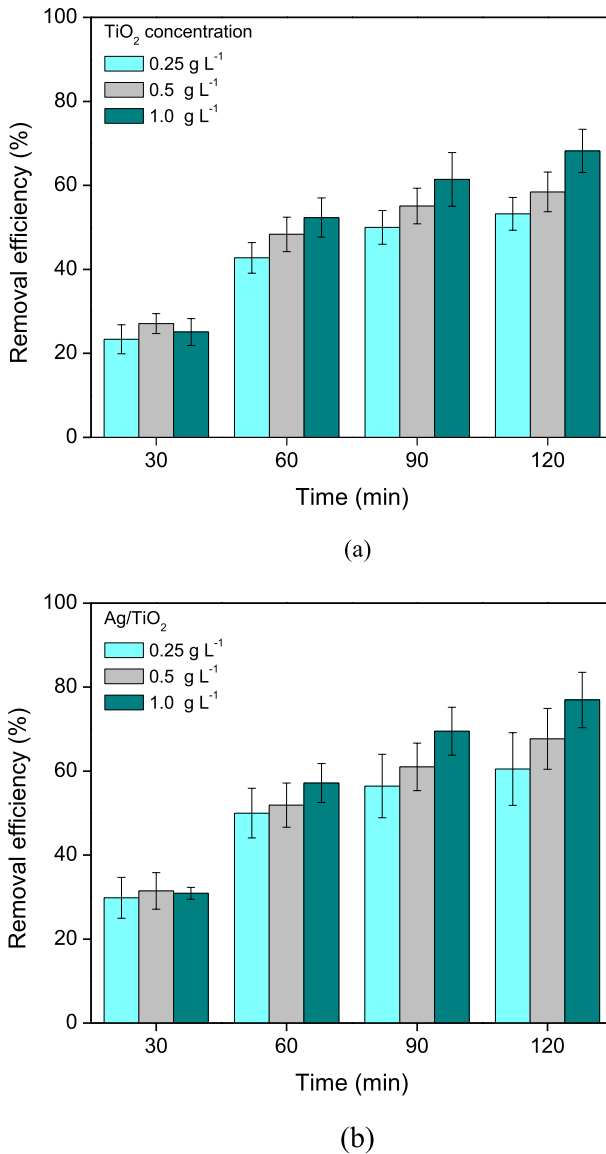


Fig. 4 Removal efficiency in the treatment of residual water by photocatalysis with **a** TiO₂ and **b** Ag/TiO₂ at different concentrations of catalyst. Experimental conditions: Hydraulic holding time: 120 min. Irradiation type: UV-C. Temperature: 25 °C. Catalyst concentrations: 0.25 g L⁻¹, 0.5 g L⁻¹, 1.0 g L⁻¹

Degradation kinetics

Table 6 shows the summary statistics obtained for the first-order exponential kinetic constant in the different treatments carried out. An analysis of variance was carried out to demonstrate the influence of different catalysts and catalyst concentrations

Table 3 Statistical summary of the results obtained through the time in the photocatalytic system with TiO₂

Time	n	Mean	Standard deviation	Coefficient of variation (%)	Min	Max	Range
Concentration of 0.25 g L ⁻¹							
0	4	124	4.32049	3.48	120	130	10
30	4	95	3.24037	3.45	91	98.5	7.5
60	4	71	2.59358	3.65	68.3	74.5	6.2
90	4	62	2.48328	4.01	59.5	65	5.5
120	4	58	2.27303	3.92	55.5	61	5.5
Concentration of 0.5 g L ⁻¹							
0	4	116.42	2.86124	2.46	113	120	7
30	4	84.9	1.97379	2.37	81	85	4
60	4	60.14	2.45764	4.09	57	63	6
90	4	52.26	2.21736	4.24	50	55	5
120	4	48.38	2.28674	4.73	45.5	51	5.5
Concentration of 1.0 g L ⁻¹							
0	4	132.18	3.06414	2.32	128.5	136	7.5
30	4	99	3.16228	3.19	95	102	7
60	4	63	2.94392	4.67	59	66	7
90	4	51	3.26599	6.40	47	55	8
120	4	42	2.16025	5.14	40	45	5

on the photocatalysis degradation rate (Table 7). The results for the pseudo-first-order degradation kinetics in the photocatalysis process were very similar to those obtained for removal efficiency. A higher degradation rate (k) was found when Ag/TiO₂ is used as a catalyst in the photocatalysis process (Fig. 5c). An increase in the degradation rate was also demonstrated when the catalyst concentration increased (Fig. 5d). This positive effect on the degradation rate of a photodegradation process was like that reported by other researchers [44]. This increase in the rate of degradation is directly related to the increase in the total surface area of the photocatalysts, that is, the number of active sites derived from a greater contact area of the surface of the catalyst nanoparticles with the contaminants. These number of active sites are available for the photocatalytic reaction as the dosage of photocatalyst increases [36, 45]. However, despite Yang et al. [44] recognized an increase in the degradation rate when TiO₂ is used in the range of 0.25 g L⁻¹ to 1.0 g L⁻¹, they also recognized that a TiO₂ concentration in excess ([TiO₂] > 1.0 g L⁻¹) did not significantly favor the removal of sulfa pharmaceuticals.

Fig. 6 shows the kinetics behavior of all treatments carried out in the photocatalytic processes with Ag/TiO₂ and TiO₂ nanoparticles. In this figure, the mean value of degradation rates can be obtained from the slope of the exponential regression equation, and is observed that the highest rates were achieved when 1.0 g L⁻¹ of both catalysts were used. The value obtained for the first-order exponential degradation constant was statistically higher when using Ag/TiO₂

Table 4 Statistical summary of the results obtained through the time in the photocatalytic system with Ag/TiO₂

Time	n	Mean	Standard deviation	Coefficient of variation (%)	Min	Max	Range
Concentration of 0.25 g L ⁻¹							
0	4	124	8.16497	6.58	118	136	18
30	4	87	4.24264	4.88	82	91	9
60	4	62	3.65148	5.89	58	66	8
90	4	54	4.08248	7.56	50	58	8
120	4	49	4.24264	8.66	44	53	9
Concentration of 0.5 g L ⁻¹							
0	4	116.4	1.9799	1.70	114.2	119	4.8
30	4	79.825	3.47215	4.35	75	83	8
60	4	56	2.94392	5.26	52	59	7
90	4	45.4	2.56645	5.65	42	48.2	6.2
120	4	37.6	2.72152	7.24	34.9	41	6.1
Concentration of 1.0 g L ⁻¹							
0	4	132.18	3.40429	2.58	128.7	136	7.3
30	4	91.3	1.28323	1.41	89.5	92.4	2.9
60	4	56.6	2.62805	4.64	53	59	6
90	4	40.3	2.30072	5.71	38	43.2	5.2
120	4	30.46	2.0025	6.58	28	32.8	4.8

Table 5 Analysis of variance for removal efficiency

Source of variation	Sum of squares	Degrees of freedom	Mean Square	F ratio	p-value
Catalyst	414.337	1	414.337	51.47	0.0000*
Concentration	1018.65	2	509.325	63.27	0.0000*
Repetition	5.6105	3	1.87017	0.23	0.8726
Error	136.854	17	8.05023		
Total	1575.45	23			

*p-value < 0.05 suggests a significant influence of the parameters on the removal efficiency

(0.013 min⁻¹) than using pure TiO₂ (0.010 min⁻¹). These results coincide with the mentioned by Diaz-Uribe et al. [46] who argued that the silver aggregates deposited on the TiO₂ surface can accumulate charge and accept electrons inside the semiconductor.

In turn, the accumulation of electrons can reduce the carrier's recombination, increasing the generation of reactive oxygen species. Hence, a collective oscillation can be caused, which is better known as localized surface plasmon resonance (SPR) [47]. The values obtained in the present study using Ag/TiO₂ are like those reported by Xu et al. [5] who obtained values of 0.017 min⁻¹ for the removal

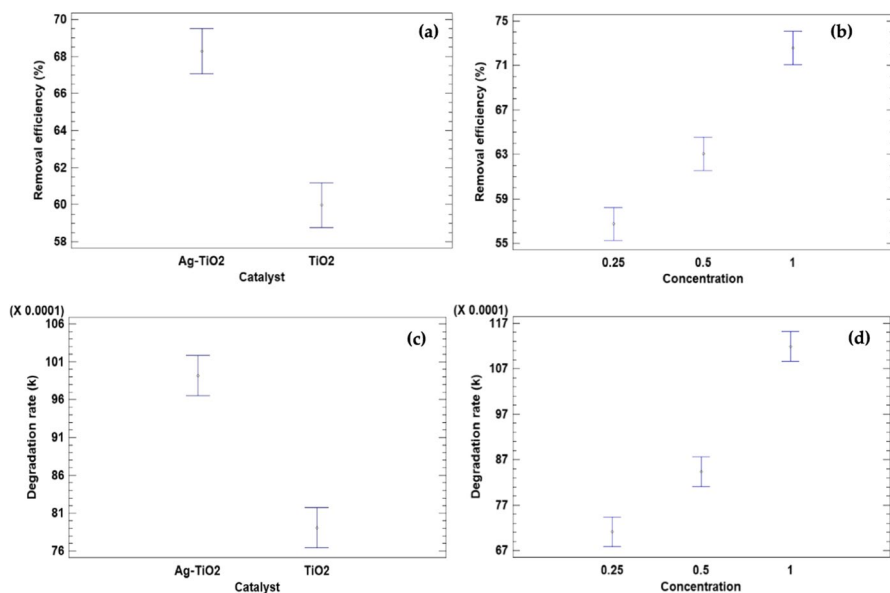


Fig. 5 LSD multiple range test for removal efficiency **a** Comparison between photocatalytic processes. **b** Comparison between catalyst concentrations. And photocatalysis degradation rate. **c** Comparison between photocatalytic processes. **d** Comparison between catalyst concentrations

Table 6 Statistical summary of the kinetic rates obtained in the present study

Treatment	Concentration g L ⁻¹	n	k (min ⁻¹)	Standard deviation	Coefficient of variation	r^2
TiO ₂	0.25	4	0.007	0.000120	1.852541	0.9605
	0.5	4	0.008	0.000306	4.120952	0.9579
	1.0	4	0.01	0.000552	5.601762	0.9851
Ag/TiO ₂	0.25	4	0.009	0.000935	12.004449	0.9564
	0.5	4	0.01	0.000537	5.698644	0.9827
	1.0	4	0.013	0.000342	2.729804	0.9959

Table 7 Analysis of variance for photocatalytic degradation rate

Source of variation	Sum of squares	Degrees of freedom	Mean Square	F ratio	p-value
Catalyst	0.0000242	1	0.000024	64.07	0.0000
Concentration	0.0000691	2	0.000035	91.51	0.0000
Repetition	0.0000005	3	0.000000	0.42	0.7418
Error	0.0000064	17	0.000000		
Total	0.0001002	23			

*p-value < 0.05 suggests a significant influence of the parameters on the photocatalytic degradation rate

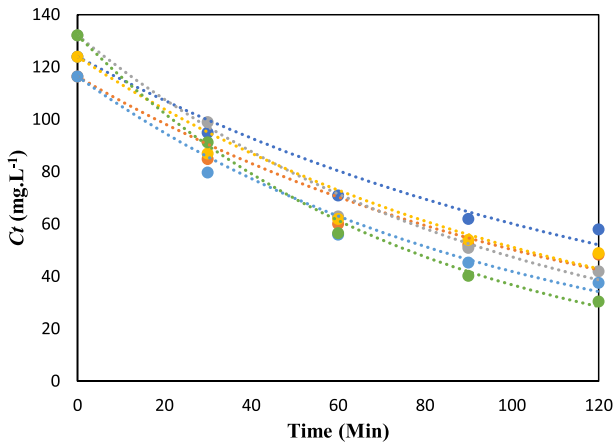


Fig. 6 Degradation rate behavior for all photocatalytic treatments for different concentrations: •TiO₂ (0.25 g.L⁻¹), •TiO₂ (0.5 g.L⁻¹), •TiO₂ (1 g.L⁻¹), •Ag/TiO₂ (0.25 g.L⁻¹), •Ag/TiO₂ (0.5 g.L⁻¹), •Ag/TiO₂ (1 g.L⁻¹). Experimental conditions: Hydraulic holding time: 120 min. Irradiation type: UV-C. Temperature: 25 °C

of atrazine through a photocatalytic oxidation process using H₃PW₁₂O₄₀/Ag-TiO₂ composite as a catalyst.

The results obtained in the present study are relevant because the present study demonstrated the feasibility of using organic matter photodegradation processes in domestic wastewater, where a great variety of contaminants is present, and a high content of solids could interfere with the photocatalysis process. In this sense, the proposed system (filter + photocatalysis) demonstrated a high removal efficiency and a high rate of organic matter degradation, which is comparable with other complex and expensive systems.

Conclusions

The technical feasibility treatment of domestic wastewater was demonstrated using a photocatalytic process with TiO₂ and Ag/TiO₂ nanoparticles. Nano-sized TiO₂ particles were synthesized using the Sol–Gel synthesis method, while Ag/TiO₂ nanoparticles were synthesized by the doping of metallic silver colloids in TiO₂ nanoparticles with a modification to the Turkevich method through chemical reduction. During the nanoparticle synthesis, the controlled variables were critical for the final particle size, which in turn plays an essential role in the photocatalytic processes. A preliminary treatment was implemented to remove the solids present in domestic wastewater. A filter comprised of zeolite, anthracite, and activated carbon was used to remove 31% of the initial solids and to avoid interfering with the further photocatalysis process. A comparison between two different catalysts (TiO₂ and Ag/TiO₂) and three different catalyst concentrations was carried out in a heterogeneous photocatalysis process. The oxidation of the organic matter present in the domestic wastewater achieved a removal efficiency of 76.96% after 2 h of photocatalysis.

The removal efficiency and degradation rate obtained in this study demonstrated a high degradation of organic pollutants in domestic wastewater, as observed in other advanced oxidation systems.

Supplementary Information The online version contains supplementary material available at <https://doi.org/10.1007/s11144-023-02557-y>.

Acknowledgements The authors thank TecNM/Instituto Tecnológico de Culiacán for providing the infrastructure to carry out this work and CONAHCYT for the scholarship provided to the first author.

Funding No funding was received for conducting this study.

Data availability Not applicable.

Declarations

Conflict of interest The author declares no competing interests.

Ethical approval Not applicable.

References

1. Bustos-Terrones Y, Estrada-Vázquez R, Ramírez-Pereda B, Bustos-Terrones V, Rangel-Peraza JG (2020) Kinetics of a fixed bed reactor with immobilized microorganisms for the removal of organic matter and phosphorous. *Water Environ Res*. <https://doi.org/10.1002/wer.1353>
2. Castillo-Ledezma JH, Salas JS, López-Malo A, Bandala ER (2011) Effect of pH, solar irradiation, and semiconductor concentration on the photocatalytic disinfection of *Escherichia coli* in water using nitrogen-doped TiO₂. *Eur Food Res Technol* 233:825
3. Rashid U, Liang H, Ahmad H, Abbas M, Iqbal A, Hamed YS (2021) Study of (Ag and TiO₂)/water nanoparticles shape effect on heat transfer and hybrid nanofluid flow toward stretching shrinking horizontal cylinder. *Results Phys* 21:103812
4. Yang H, Wang Y, Xue X (2014) Influences of glycerol as an efficient doping agent on crystal structure and antibacterial activity of B-TiO₂ nano-materials. *Colloids Surf B: Biointerfaces* 122:701–708
5. Xue X, Wang Y, Yang H (2013) Preparation and characterization of boron-doped titania nano-materials with antibacterial activity. *Appl Surf Sci* 264:94–99
6. Peiris S, de Silva HB, Ranasinghe KN, Bandara SV, Perera IR (2021) Recent development and future prospects of TiO₂ photocatalysis. *J Chin Chem Soc* 68:738–769
7. Ijaz M, Zafar M (2021) Titanium dioxide nanostructures as efficient photocatalyst: progress, challenges and perspective. *Int J Energy Res* 45:3569–3589
8. Losada LM, Laguna Castillo EJ, Osorio Restrepo EA, Serna Galvis EA, Torres Palma RA (2017) Tratamiento de aguas contaminadas con colorantes mediante fotocatalisis con TiO₂ usando luz artificial y solar. *Prod Limpia* 12(2):50–60
9. Fernández JA, Cardozo MG, Carrascal AK, Salcedo JC, Pedroza AM, Daza CE (2015) Tratamiento de agua residual de microbiología usando películas delgadas de TiO₂. *Ing Compet* 17:35–48
10. Dodoo-Arhin D, Buabeng FP, Mwabora JM, Amaniampong PN, Agbe H, Nyankson E, Asiedu NY (2018) The effect of titanium dioxide synthesis technique and its photocatalytic degradation of organic dye pollutants. *Heliyon* 4:e00681
11. Bibi S, Shah S, Muhammad F, Siddiq M, Kiran L, Aldossari A, Sarwar S (2023) Cu-doped mesoporous TiO₂ photocatalyst for efficient degradation of organic dye via visible light photocatalysis. *Chemosphere* 339:139583
12. Tobaldi DM, Pullar RC, Gualtieri AF, Seabra MP, Labrincha JA (2013) Sol–gel synthesis, characterisation and photocatalytic activity of pure, W-, ag- and W/Ag co-doped TiO₂ nanopowders. *Chem Eng Technol* 214:364–375

13. Wang Y, Wu Y, Yang H, Xue X, Liu Z (2016) Doping TiO₂ with boron or/and cerium elements: effects on photocatalytic antimicrobial activity. *Vacuum* 131:58–64
14. Wang Y, Xue X, Yang H (2014) Preparation and characterization of carbon or/and boron-doped titania nano-materials with antibacterial activity. *Ceram Int* 408:12533–12537
15. Wang L, Ali J, Zhang C, Mailhot G, Pan G (2020) Simultaneously enhanced photocatalytic and antibacterial activities of TiO₂/Ag composite nanofibers for wastewater purification. *J Environ Chem Eng* 8:102104
16. Ghosh M, Mondal M, Mandal S, Roy A, Chakrabarty S, Chakrabarti G, Pradhan SK (2020) Enhanced photocatalytic and antibacterial activities of mechanothesized TiO₂-Ag nanocomposite in wastewater treatment. *J Mol Struct* 1211:128076
17. Athanasekou C, Romanos GE, Papageorgiou SK, Manolis GK, Katsaros F, Falaras P (2017) Photocatalytic degradation of hexavalent chromium emerging contaminant via advanced titanium dioxide nanostructure. *Rev Ing Quim* 318:171–180
18. Subekti R, Helmiyati H (2020) Sodium alginate-TiO₂-bentonite nanocomposite synthesis for photocatalysis of methylene blue dye removal. *IOP Publishing* 763:012018
19. Domínguez-Espíndola RB, Varia JC, Álvarez-Gallegos A, Ortiz-Hernández ML, Peña-Camacho JL, Silva-Martínez S (2017) Photoelectrocatalytic inactivation of fecal coliform bacteria in urban wastewater using nanoparticulated films of TiO₂ and TiO₂/Ag. *Environ Technol* 38:606–614
20. Nguyen CH, Fu CC, Juang RS (2018) Degradation of methylene blue and methyl orange by palladium-doped TiO₂ photocatalysis for water reuse: efficiency and degradation pathways. *J Clean Prod* 202:413–427
21. De la Cruz RD, Torres GT, Arévalo JC, Gomez R, Aguilar-Elguezabal A (2010) Synthesis and characterization of TiO₂ doping with rare earths by sol-gel method: photocatalytic activity for phenol degradation. *J Sol-Gel Sci Technol* 56:219–226
22. Xu L, Zang H, Zhang Q, Chen Y, Wei Y, Yan J, Zhao Y (2013) Photocatalytic degradation of atrazine by H₃PW₁₂O₄₀/Ag-TiO₂: kinetics, mechanism and degradation pathways. *Chem Eng Technol* 232:174–182
23. Panayotov DA, Morris JR (2016) Surface chemistry of Au/TiO₂: thermally and photolytically activated reactions. *Surf Sci Rep* 71:77–271
24. Alarifi A, Deraz NM, Shaban S (2009) Structural, morphological and magnetic properties of NiFe₂O₄ nano-particles. *J Alloys Compd* 486:501–506
25. Ramos D, Bezerra PC, Quina FH, Dantas RF, Casagrande GA, Oliveira SC, Machulek A (2015) Synthesis and characterization of TiO₂ and TiO₂/Ag for use in photodegradation of methylviologen, with kinetic study by laser flash photolysis. *Environ Sci Pollut Res Int* 22:774–783
26. Sagadevan S, Pal K, Koteeswari P, Subashini A (2017) Synthesis and characterization of TiO₂/graphene oxide nanocomposite. *J Mater Sci: Mater Electron* 28:7892–7898
27. Chatzisymeon E, Droumpali A, Mantzavinos D, Venieri D (2011) Disinfection of water and wastewater by UV-A and UV-C irradiation: application of real-time PCR method. *Photochem Photobiol Sci* 10:389–395
28. Bockenstedt J, Vidwans NA, Gentry T, Vaddiraju S (2021) Catalyst recovery, regeneration and reuse during large-scale disinfection of water using photocatalysis. *Water* 13(19):2623
29. Roulová N, Hrdá K, Kašpar M, Peroutková P, Josefová D, Palarčík J (2022) Removal of chloroacetanilide herbicides from water using heterogeneous photocatalysis with TiO₂/UV-A. *Catalysts* 12(6):597
30. Jamshidi F, Dehghani M, Yousefinejad S, Azhdarpoor A (2019) Photocatalytic degradation of alachlor by TiO₂ nanoparticles from aqueous solutions under UV radiation. *J Exp Nanosci* 14(1):116–128
31. Ren M, Qu G, Li H, Ning P (2019) Influence of dissolved organic matter components on arsenate adsorption/desorption by TiO₂. *J Hazard Mater*. <https://doi.org/10.1016/j.jhazmat.2019.120780>
32. Safari GH, Hoseini M, Seyedsalehi M, Kamani H, Jaafari J, Mahvi AH (2015) Photocatalytic degradation of tetracycline using nanosized titanium dioxide in aqueous solution. *Int J Environ Sci Technol* 12:603–616
33. Lente G (2015) *Deterministic kinetics in chemistry and systems biology: the dynamics of complex reaction networks*. Springer, New York
34. Estrada-Vázquez R, Vaca-Mier M, Bustos-Terrones V, Rangel-Peraza JG, Loaiza JG, Hermosillo-Nevárez JJ, Bustos-Terrones YA (2023) Degradation of agricultural pollutants by biopolymer-enhanced photocatalysis: application of Taguchi method for optimization. *Kinet Mech Catal React*. <https://doi.org/10.1007/s11144-023-02515-8>

35. Martínez-Rojas V, Matejova L, López-Milla A, Cruz GJ, Solís Veliz JL, Gomez Leon MM (2015) Obtención de partículas de TiO₂ por sol-gel, asistido con ultrasonido para aplicaciones fotocatalíticas. *Revista de la Sociedad Química del Perú*. <https://doi.org/10.37761/rsqp.v8i13.17>
36. Al Qarni F, Alomair N, Mohamed H (2019) Environment-friendly nanoporous titanium dioxide with enhanced photocatalytic activity. *Catalysts*. <https://doi.org/10.3390/catal9100799>
37. Echavarría AM, Robledo S, Bejarano G (2017) Influencia de las nanopartículas de Ag sobre las propiedades mecánicas y tribológicas y en el efecto citotóxico y bactericida de los recubrimientos de TaN (Ag). *Rev de Metal* 53:e085
38. Komaraiah D, Radha E, Sivakumar J, Reddy MR, Sayanna R (2020) Photoluminescence and photocatalytic activity of spin coated Ag⁺ doped anatase TiO₂ thin films. *Opt Mater* 108:110401
39. Pinto VV, Ferreira MJ, Silva R, Santos HÁ, Silva F, Pereira CM (2010) Long time effect on the stability of silver nanoparticles in aqueous medium: effect of the synthesis and storage conditions. *Colloids Surf A* 364:19–25
40. Barrientos KC, Iparraguirre DEA, Cavero HAA (2019) Síntesis y caracterización de nanocompuestos Fe₃O₄/Ag: su efecto contra *Enterobacter aerogenes* y *Enterococcus faecalis*. *Rev Colomb Quím* 48:33–39
41. Ramacharyulu PV, Praveen-kumar J, Prasad GK, Srivastava AR (2015) Synthesis, characterization and photocatalytic activity of Ag-TiO₂ nanoparticulate film. *RSC Adv* 5:139–1314
42. Pragathiswaran C, Smitha C, Abbubakkar BM, Govindhan P, Krishnan NA (2021) Synthesis and characterization of TiO₂/ZnO–Ag nanocomposite for photocatalytic degradation of dyes and antimicrobial activity. *Mater Today* 45:3357–3364
43. Haider AJ, AL Anbari RH, Kadhim GR, Salame CT (2017) Exploring potential environmental applications of TiO₂ nanoparticles. *Energy Procedia* 119:332–345
44. Yang H, Li G, An T, Gao Y, Fu J (2010) Photocatalytic degradation kinetics and mechanism of environmental pharmaceuticals in aqueous suspension of TiO₂: a case of sulfa drugs. *Catal Today* 153:200–207
45. Lusvardi G, Barani C, Giubertoni F, Paganelli G (2017) Synthesis and characterization of TiO₂ nanoparticles for the reduction of water pollutants. *Materials* 10:1208
46. Diaz-Urbe C, Vilorio J, Cervantes L, Vallejo W, Navarro K, Romero E, Quiñones C (2018) Photocatalytic activity of Ag-TiO₂ composites deposited by photoreduction under UV irradiation. *Int J Photoenergy* 6080432:1–8
47. Torrell M, Kabir R, Cunha L, Vasilevskiy MI, Vaz F, Cavaleiro A, Barradas NP (2011) Tuning of the surface plasmon resonance in TiO₂/Au thin films grown by magnetron sputtering: the effect of thermal annealing. *Int J Appl Phys* 109:074310

Publisher's Note Springer Nature remains neutral with regard to jurisdictional claims in published maps and institutional affiliations.

Springer Nature or its licensor (e.g. a society or other partner) holds exclusive rights to this article under a publishing agreement with the author(s) or other rightsholder(s); author self-archiving of the accepted manuscript version of this article is solely governed by the terms of such publishing agreement and applicable law.